Contents lists available at ScienceDirect

Journal of Magnetism and Magnetic Materials

Exchange bias in Co/CoO/Co$_3$O$_4$ nanostructures

Hossein Ahmadvand [a,*], Sayed Reza Safdari [a], Ahmad Nozad Golikand [b], Papri Dasgupta [c], Asok Poddar [c], Hadi Salamati [a]

[a] Department of Physics, Isfahan University of Technology, Isfahan 84156-83111, Iran
[b] Material Research Center, Isfahan 81465-1589, Iran
[c] Saha Institute of Nuclear Physics, 1/AF Bidhannagar, Kolkata 700064, India

ARTICLE INFO

ABSTRACT

Nanostructures of Co/CoO/Co$_3$O$_4$ were synthesized by a chemical method at different temperatures between 300 and 600 °C. The samples were characterized by TG, XRD, TEM and SQUID magnetometry. The lower temperature sample (300 °C) is composed of Co, CoO and Co$_3$O$_4$, while the higher temperature sample only contains Co$_3$O$_4$. All the samples exhibit exchange bias effect. The exchange bias is observed below 205 K (below the CoO blocking temperature) for the sample prepared at lower temperature (300 °C), while for other samples (350–600 °C), the effect is observed below 35 K (below the Néel temperature of Co$_3$O$_4$, $T_N = 40$ K). The roles of CoO and Co$_3$O$_4$ on the magnetic properties and the mechanisms governing exchange bias effect have been discussed.

© Elsevier B.V. All rights reserved.

1. Introduction

Exchange bias effect was first discovered in 1956–1957 by Meiklejohn and Bean in fine ferromagnetic (FM) Co particles with a shell of antiferromagnetic (AFM) CoO [1]. This effect is the shift of hysteresis loop along the field axis and usually appears when FM/AFM hybrid system is cooled below the AFM Néel temperature in the presence of an external magnetic field. Since its discovery, extensive research has been devoted to exploring and understanding the exchange bias in many different systems such as bilayers, core-shell nanoparticles and inhomogeneous materials [2,3]. The exchange bias effect has been extensively reported in Co/CoO [4,5] and rarely reported in Co/Co$_3$O$_4$ bilayer thin film [6,7]. This effect has been also observed in Co$_3$O$_4$ nanostructures [8–10] in which the FM part comes from the particles/nanowires surface. In this study, we report the exchange bias in a nanostructure containing both AFM cobalt oxides (CoO and Co$_3$O$_4$).

2. Experimental

The Co/CoO/Co$_3$O$_4$ nanostructures were prepared by a method which was previously used for synthesizing NiO and Ni/NiO nanoparticles [11,12]. High purity cobalt (II) acetate tetrahydrate, 2-methoxy ethanol, N,N-dimethylformamide and polyvinyl acetate (PVAc) (molecular weight 55,000–70,000) were used as raw materials. The nanostructure was prepared as follows: 0.1 mol cobalt (II) acetate tetrahydrate was dissolved in 1 mol 2-metoxy ethanol by heating and stirring at 70 °C for 2 h (solution A). Polyvinyl acetate (14 wt%) solution was prepared in N,N-dimethyl-formamide by stirring at room temperature (solution B). A mixture of solutions A and B in the ratio of 1:4 was prepared by stirring at room temperature for 3 h. Then, the obtained solution was rapidly heated to 150 °C and kept at this temperature to remove the solvent. Finally, the dried solid precursor was well ground and calcined at different temperatures 300 (S300), 350 (S350), 400 (S400), 450 (S450) and 600 °C (S600) for 3 h to obtain Co/Co-oxide nanocrystalline samples.

The thermal behavior of the dried precursor was studied by thermogravimetry (TG) and differential scanning calorimetry (DSC). Structural characterization was performed by X-ray powder diffraction (XRD) with Cu $K\alpha$ radiation. The morphology and particle size were examined by transmission electron microscopy (TEM) images. Magnetic measurements were carried out using a superconducting quantum interference device (SQUID) magnetometer (Model SVSM 7).

3. Results and discussion

Fig. 1 shows the TG and DSC curves for the dried solid precursor. The two-step weight losses (300–500 °C) in the TG curve are due to the decomposition of PVAc [13]. PVAc starts
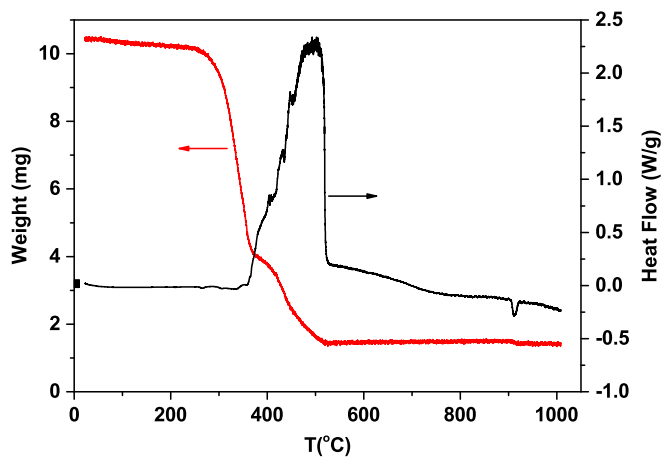
Fig. 1. TG-DSC analysis of the dried precursor.

decomposing at about 300 and the process is completed at about 520 °C leaving Co_3O_4 as the end product. The small endothermic peak at 910 °C is due to the conversion of Co_3O_4 to CoO. The XRD patterns of the samples (calcined between 300 and 600 °C) are shown in Fig. 2. It is found that the main phase of all samples is Co_3O_4 with a normal spinel crystal structure. In addition to the main phase, there are small peaks related to CoO. The CoO peaks decreases with increasing calcination temperature and disappear in sample S600. Sample S600 has a single Co_3O_4 phase. There are no peaks related to Co in the XRD patterns. Nevertheless, magnetic measurements reveal the presence of Co in the low temperature calcined samples. Fig. 3 shows typical TEM images of samples S300, S400 and S600. The average particle size was estimated to be about 30, 50 and 65 nm, respectively. From the above discussion, it can be concluded that the samples are inhomogeneously composed of Co, CoO and Co_3O_4 nanocrystals, probably with residual PVAc.

Temperature dependence of field cooled (FC) and zero field cooled (ZFC) magnetization was performed at a low (100 or 114 Oe) and at a relatively high (5 kOe) magnetic field. The results are presented in Fig. 4. It is seen that two peaks appear in the ZFC magnetization at about ~295 and 40 K, which are related to the Néel temperatures of CoO and Co_3O_4 respectively. For sample S600 (Fig. 4(e)) the peak at 295 K is not seen indicating the absence of CoO phase. As Fig. 4(a)–(e) shows, at low magnetic field, a pronounced irreversibility is observed between the ZFC and FC
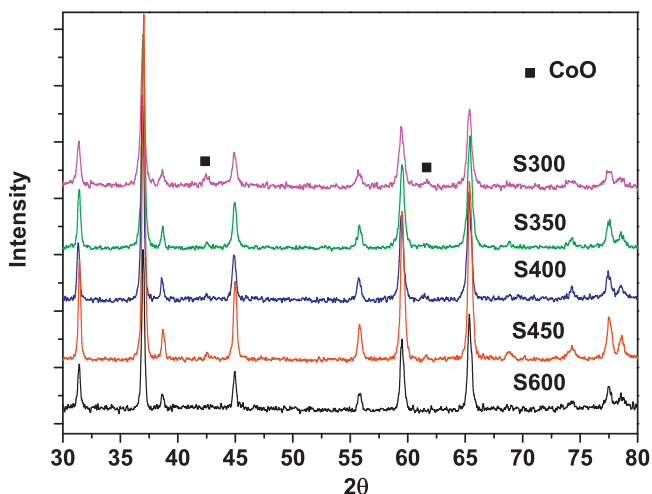

Fig. 2. XRD patterns of the samples prepared at different temperatures. Solid squares denote the peaks of CoO and the other peaks are assigned to Co_3O_4.

curves which decreases with increasing calcination temperature and becomes very small for sample S600. In the presence of a high magnetic field of 5 kOe (Fig. 4(f)), only the Néel transition of Co_3O_4 at 40 K is seen and the FC/ZFC irreversibility vanishes except for sample S300. For S300, the FC and ZFC magnetizations begin to separate below $T_{irr} \simeq 240$ K. Such irreversibility is a signature of a blocking process in the sample.

In order to further study the magnetic properties of the samples, we measured the FC and ZFC hysteresis loops at different temperatures between 5 K and room temperature. The ZFC M–H loops taken at 5 K are shown in Fig. 5. The loop of sample S300 taken at 285 K is also presented in the inset of Fig. 5. As can be seen, the magnetization decreases with increasing calcination temperature. Moreover, the central part of the loops of sample S300 is similar to a FM-type, while the loop of sample S600 is linear characteristic of the AFM state. The FM part in sample S300 indicates the presence of a small amount of metallic cobalt which is eliminated by increasing calcination temperature in sample S600. The FC hysteresis loops were measured after cooling the samples from 320 K under an applied field of 50 kOe. The loops are shifted along the field axis, demonstrating that exchange bias has been established in all the samples. As examples, Fig. 6 shows the FC and ZFC loops of samples S300 and S600 taken at 5 K which exhibit an exchange bias field (H_E) of about 397 and 131 Oe, respectively. The temperature dependence of H_E, FC coercivity ($H_C(FC)$) and ZFC coercivity ($H_C(ZFC)$) for sample S300 is presented in Fig. 7(a). The H_E versus temperature for other samples is shown in Fig. 7(b). The important point is that the exchange bias in sample S300 is observed below the irreversibility temperature (see Fig. 4(f)), while in the other samples is observed below 40 K (the Néel transition of Co_3O_4). Moreover, as Fig. 7(a) shows, the exchange bias in sample S300 is accompanied with an enhancement of coercivity which is a characteristic of exchange bias systems.

The existence of exchange bias above 40 K in sample S300 lead us to conclude that there are Co(FM)/CoO(AFM) interfaces with exchange coupling in this sample. Such interfaces are not present or not effective to produce exchange bias above 40 K in the other samples. This fact is consistent with the M–T data of the samples presented in Fig. 4(f) in which the FC/ZFC irreversibility at a field of 5 kOe is only observed in sample S300. In fact, the irreversibility temperature at about $T_{irr} \simeq 240$ K is the exchange bias blocking temperature above which the exchange bias effect disappears. In this system, the blocking behavior is mainly attributed to CoO crystallites, because Co in sample S300 is in the ferromagnetism state above T_{irr} (see inset of Fig. 5). The irreversibility between FC and ZFC magnetization is more pronounced below T_N of CoO indicates the role of CoO in the irreversibility behavior. In fact, as discussed by Peng et al. the irreversibility temperature is mainly determined by the anisotropy of the AFM CoO shell rather than the intrinsic anisotropy of the Co core [5].

The exchange bias in Co/Co_3O_4 bilayers was previously observed below 220 [7] and 240 K [6]. The authors showed that a thin CoO layer formed at the interface between Co and Co_3O_4 which induces exchange bias in the system above 40 K. Moreover, it is reported that in oxidized cobalt particles, the CoO phase is found on the surface of the Co particles, forming a shell and the Co_3O_4 phase often occurs at junctions of particles in fractals [14]. Therefore, it is not unreasonable to expect that in sample S300, the CoO phase is formed between Co and Co_3O_4 and leads to the formation of Co/CoO/Co_3O_4 nanostructure. As Fig. 7(a) shows, interestingly all the H_E, $H_C(FC)$ and $H_C(ZFC)$ are enhanced below 40 K. This enhancement may be related to the coupling between CoO and Co_3O_4 which enhances the anisotropy of CoO. However, there is a faint possibility to have distinct Co/CoO and Co/Co_3O_4 interfaces in the sample.